

BLUE-SKY CATASTROPHE IN SINGULARLY PERTURBED SYSTEMS

ANDREY SHILNIKOV, LEONID SHILNIKOV, AND DMITRY TURAEV

Dedicated to Yu. S. Ilyashenko on the occasion of his 60th birthday

ABSTRACT. We show that the blue-sky catastrophe, which creates a stable periodic orbit of unboundedly increasing length, is a typical phenomenon for singularly perturbed (multi-scale) systems with at least two fast variables. Three distinct mechanisms of this bifurcation are described. We argue that it is behind the transition from periodic spiking to periodic bursting oscillations.

2000 MATH. SUBJ. CLASS. 37G15, 34E15, 37C27, 34C26.

KEY WORDS AND PHRASES. Saddle-node, global bifurcations, stability boundaries, slow-fast system, bursting oscillations, spikes, excitability.

1. STABILITY BOUNDARIES FOR PERIODIC ORBITS

Stable periodic orbits play a very special role in nonlinear dynamics. One of the basic questions here concerns the structure of the boundaries of their stability regions in the parameter space. Namely, suppose that a time-continuous dynamical system exhibits sustainable self-oscillations, i. e., has a stable periodic orbit. The question is: How do the periodic orbits evolve as the parameters of the system vary? In other words, consider a one-parameter family X_μ of dynamical systems with an exponentially stable periodic orbit at some μ . This periodic orbit will persist and remain stable within some interval of parameter values. What is the boundary of this interval? Which type of bifurcation does correspond to it in a typical one-parameter family?

These questions gave an initial impulse to the development of bifurcation theory in the pioneering works by Andronov and Leontovich [1] (see also [2]), who discovered the following four codimension-1 boundaries of stability of limit cycles for systems of ODEs in the plane. The first one corresponds to a stable limit cycle bifurcating from/into a stable equilibrium state; on the second boundary, a stable limit cycle coalesces with an unstable one and disappears; on the third boundary, a

Received April 23, 2003.

Supported by the RFBR Grants Nos. 05-01-00558, 02-01-00273 and 01-01-00975, INTAS Grant No. 2000-221, and program “Universities of Russia”, project No. 1905. The second-named author acknowledges the support of the Alexander von Humboldt foundation.

periodic orbit transforms into a homoclinic loop of a simple saddle-node equilibrium state; the last, fourth, boundary corresponds to a stable periodic orbit becoming a homoclinic orbit to a saddle equilibrium state with negative saddle value.

In the multi-dimensional case, seven stability boundaries for generic one-parameter families are known at present. They are divided into two types depending on whether or not the periodic orbit under consideration exists at the critical moment. In the former case, the intersection of the periodic orbit with a local cross-section is the fixed point of the Poincaré map, so the problem reduces to the analysis of how the multipliers of the fixed point exit the unit circle. The first possibility is similar to the two-dimensional case: a single multiplier of the periodic orbit becomes equal to $+1$; this is the *saddle-node* bifurcation (see Fig. 1). The two remaining codimension-1 bifurcations are the flip or period-doubling bifurcation and the birth of a torus. At a flip bifurcation point, there is a single multiplier equal to -1 . The periodic orbit itself does not disappear after this bifurcation (unlike in the saddle-node case) but only loses stability. In the case where a pair of complex-conjugate multipliers crosses the unit circle outward, the periodic orbit survives too, but it loses its skin: a stable two-dimensional invariant torus is born.

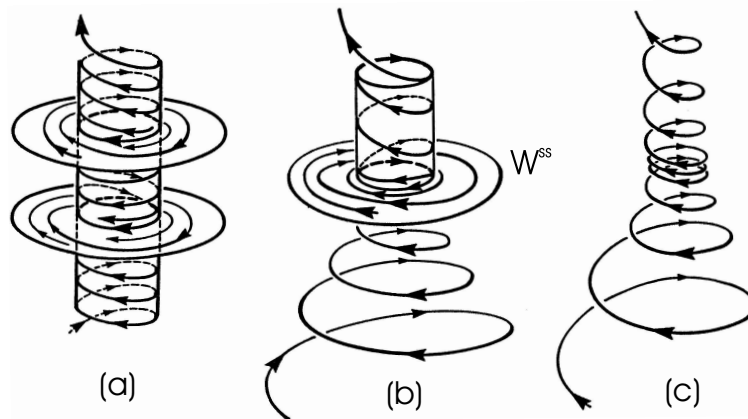


FIGURE 1. Saddle-node bifurcation: (a) $\mu < 0$, there are two periodic orbits: stable and saddle; (b) $\mu = 0$, the periodic orbits merge into a saddle-node orbit. Its strong stable manifold W^{ss} divides the neighborhood into the node region (below W^{ss} in the figure) and the saddle region (above W^{ss}). The unstable manifold is the part of the center manifold which lies in the saddle region; (c) $\mu > 0$, the saddle-node disappears; the drifting time through its neighborhood is estimated as $\sim 1/\sqrt{\mu}$.

There are three stability boundaries of the second kind, as in the planar case. They correspond to the birth of a periodic orbit off a stable equilibrium state (the Andronov–Hopf bifurcation) and to its flowing into a homoclinic loop of either a simple saddle-node equilibrium state or a hyperbolic equilibrium state with one-dimensional unstable manifold and with negative saddle value [8].

It can be shown that the above list gives *all* the main stability boundaries for the case where the *length* of the periodic orbit remains bounded at the bifurcation moment (although the period may tend to infinity if the orbit adheres to a homoclinic loop). One more (and, *conjecturally*, the last one) main boundary of stability that has no two-dimensional analogues and corresponds to the unbounded growth of the length of the periodic orbit was discovered in [13]. This is a codimension-1 bifurcation of smooth flows in at least three-dimensional phase space such that, for any one-parameter family X_μ of flows which crosses the corresponding bifurcation surface at, say, $\mu = 0$ and for all small $\mu > 0$ (with an appropriate choice of the direction of increasing the parameter μ), the flow has a stable periodic orbit L_μ which remains in a bounded region of the phase space and is away from any equilibrium states; besides, it undergoes no bifurcations as $\mu \rightarrow +0$, whereas both its period and length increase without bound, and L_μ disappears at $\mu = 0$.

The existence of such type of bifurcations (called the blue-sky catastrophe) was a long-standing problem. In the construction suggested in [13] (see also [11], [12], [9]), the blue-sky stability boundary is an open subset of a codimension-1 bifurcation surface corresponding to the existence of a saddle-node periodic orbit. This open set is distinguished by some qualitative conditions that determine the geometry of the unstable manifold of the saddle-node (see Fig. 2) and by a few quantitative restrictions (the Poincaré map introduced below must be a contraction). If all the required conditions hold, then the stable periodic orbit L_μ whose period and length both tend to infinity when approaching the moment of bifurcation is born when the saddle-node orbit disappears.

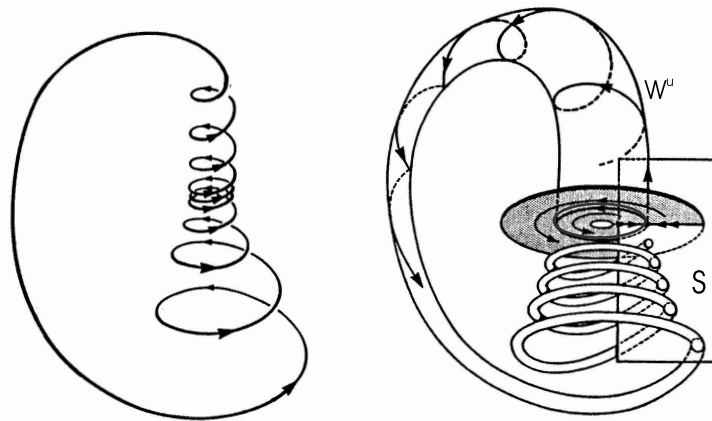


FIGURE 2. The global structure of the set W^u for the blue-sky catastrophe. The intersection of W^u with the local cross-section S in the node region is a countable set of circles accumulating to $S \cap L$.

The global structure of the unstable set of the saddle-node for the blue-sky catastrophe appears to be rather complex, and hence it may be unclear how this construction can be achieved in dynamical systems of a natural origin; nevertheless,

the answer was promptly. The first explicit example of a three-dimensional system of ODEs where the blue-sky catastrophe occurs was constructed in [5] considering a global homoclinic Guckenheimer–Gavriloﬀ bifurcation with an extra degeneracy. Another setup for the blue-sky bifurcation was proposed in [9], where it was shown that this particular configuration of the unstable set of the saddle-node is, in fact, quite typical for slow-fast (i.e., singularly perturbed) systems with at least two fast variables. In this paper, we present and analyze specific scenarios which cause indeed the blue-sky catastrophe in singularly perturbed systems.

2. SLOW-FAST SYSTEMS

A slow-fast system is a system of the form

$$\begin{aligned} \dot{x} &= g(x, y, \varepsilon), \\ \varepsilon \dot{y} &= h(x, y, \varepsilon), \end{aligned} \tag{1}$$

where $\varepsilon > 0$ is a small parameter. This system can be regularized by rescaling the time $t = \varepsilon\tau$. With the new time τ , system (1) becomes

$$\begin{aligned} x' &= \varepsilon g(x, y, \varepsilon), \\ y' &= h(x, y, \varepsilon), \end{aligned} \tag{2}$$

where the prime denotes differentiating with respect to τ . Taking the limit as $\varepsilon \rightarrow 0$, we obtain

$$\begin{aligned} x' &= 0, \\ y' &= h(x, y, 0). \end{aligned} \tag{3}$$

The second equation here is called the *fast* system. For simplicity, we assume that $x \in \mathbb{R}^1$. The variable x can be considered as a parameter which governs the motion of the fast y -variables; we assume that $y \in \mathbb{R}^n$, where $n \geq 2$.

A trajectory of system (3) starting off any initial point (x, y) goes typically to an attractor of the fast system for the given value of x . The attractor may be a stable equilibrium, or a stable periodic orbit, or have a less trivial structure; we would like to leave out a discussions of the last possibility for now. When the equilibrium state or the periodic orbit of a fast system is exponentially stable, it depends smoothly on x . Thus, we obtain a smooth attracting invariant manifold of system (3): the equilibria of the fast system form curves M_{eq} in the (x, y) -space, while the limit cycles form two-dimensional cylinders M_{po} ; see Fig. 3.

Locally, near any exponentially stable equilibrium point or a periodic orbit of the fast subsystem, such a manifold is a center manifold for system (3). Since the center manifold persists for any close system, it follows that the smooth attractive invariant manifolds $M_{\text{eq}}(\varepsilon)$ and $M_{\text{po}}(\varepsilon)$ exist for all small ε in the whole system (2) (see [3], [4] for details).

Thus, any trajectory of system (2) for small $\varepsilon > 0$ behaves in the following way: in a finite time, it enters a small neighborhood of one of the invariant manifolds M_{eq} and M_{po} so that its x -component remains nearly constant. Then, it begins drifting slowly along the chosen invariant manifold with the rate of change of x of order ε .

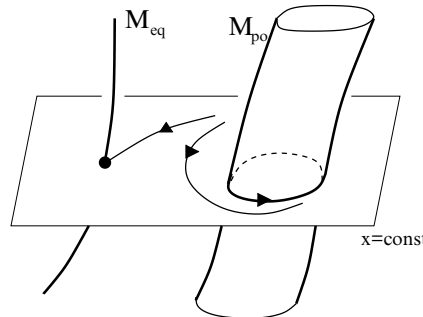


FIGURE 3. An orbit of a fast subsystem can tend to a stable equilibrium or to a stable limit cycle.

In the original system (1) in contrast with the above development, an almost instant jump in the y -components towards the invariant manifold followed by a finite speed motion in the x -variable occurs. In addition, if this is the manifold M_{po} , then a fast circular motion in the y -components, as shown in Fig. 4, is observed.

The equilibrium states of the fast system are found from the condition $h(x, y, 0) = 0$, which yields the algebraic equation for M_{eq} . If $y = y_{eq}(x)$ is a stable branch of M_{eq} , then the equation of motion of the x -component along it is given, up to the first order in ε , by

$$\dot{x} = g(x, y_{eq}(x), 0). \tag{4}$$

This is a one-dimensional system which may possess attracting and repelling equilibrium states corresponding to stable and saddle equilibrium states in the entire system (1) or (2). Either the evolution along M_{eq} is limited to one of the stable points or the trajectory hovers about M_{eq} onwards until it reaches a small neighborhood of a critical value of x . Recall that x is treated as a governing parameter for the fast system, and hence its critical values correspond to bifurcations in the fast system. For instance, at such a critical value x^* , two, stable and unstable, equilibrium states of the fast subsystem may collide, thereby forming a saddle-node. This corresponds to a maximum (or a minimum) of x on M_{eq} . The x -component of the trajectory can no longer increase (respectively, decrease) along the stable branch of M_{eq} . Instead, the orbit jumps towards another attractor, which is the ω -limit set of the outgoing separatrix of the saddle-node equilibrium state in the fast system at $x = x^*$; see Fig. 5.

In order to determine the dynamics of the trajectory near the cylinder $M_{po}(\varepsilon)$, we must first find the equation $y = y_{po}(\tau; x)$ of the corresponding fast limit cycle for the given x ; here y_{po} is a periodic function in τ of period $T(x)$. Then, we substitute $y = y_{po}(t\varepsilon; x)$ into the right-hand side of the first equation in (1) and average it over the period $T(x)$. The resulting averaged system

$$\dot{x} = \phi(x) \equiv \frac{1}{T(x)} \int_0^{T(x)} g(x, y_{po}(\tau; x), 0) d\tau \tag{5}$$

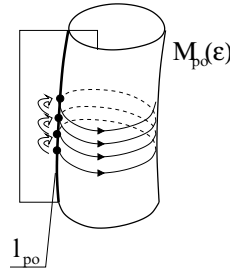


FIGURE 4. The fast circular motion on the cylinder $M_{po}(\epsilon)$ defines the Poincaré map of the intersection curve $l_{po}(\epsilon)$.

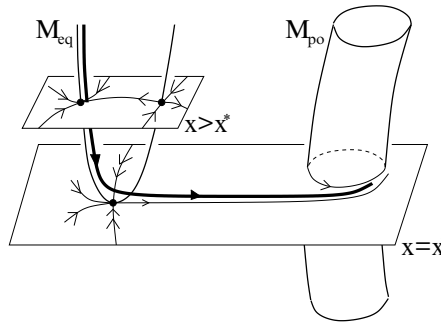


FIGURE 5. The fast jump of a trajectory from the fold towards the attracting cylindrical surface.

gives a first-order approximation (see [6]) for the evolution of the x -component of the orbit near M_{po} .

Cutting the cylinder surface by a cross-section transverse to the fast motion (see Fig. 4), we find a Poincaré map defined on the intersection line $l_{po}(\epsilon)$:

$$\bar{x} = x + \varepsilon\psi(x, \varepsilon) = x + \varepsilon\phi(x)T(x) + o(\varepsilon). \tag{6}$$

This one-dimensional map may have stable and unstable fixed points (at the zeros of $\psi(x)$). These points correspond to stable and saddle periodic orbits of system (1). The iterates of any point on l_{po} either converge to one of the stable fixed points of the map or continue to grow monotonically up to the critical value of x .

A critical value of x corresponds to a bifurcation in the fast system. We shall consider three types of such bifurcations. The first one (see Fig. 6) corresponds to the case where the stable periodic orbit of the fast system collides with a saddle periodic orbit, forming thereby a saddle-node one, which then fades. After passing such a critical value, the orbits of the singularly-perturbed system (1) must follow orbits of the fast subsystem, i. e., they jump toward the ω -limit set of the unstable manifold of the saddle-node.

The second situation illustrated in Fig. 7 corresponds to the case where the stable periodic orbit of the fast system shrinks to a focus. After passing through

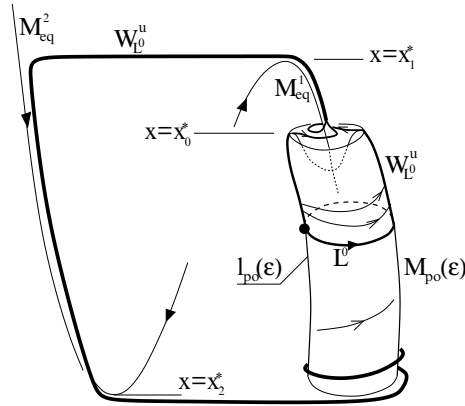


FIGURE 6. The fold on M_{po} (due to the saddle-node bifurcation in the fast system at $x = x_0^*$) triggers the fast jump towards the attracting slow-motion surface M_{eq}^1 corresponding to equilibria of the fast subsystem. The unstable manifold of the saddle-node periodic orbit L^0 shrinks to a narrow tube after the jump.

the critical value, the phase point drifts along the corresponding branch of stable equilibria of the fast system.

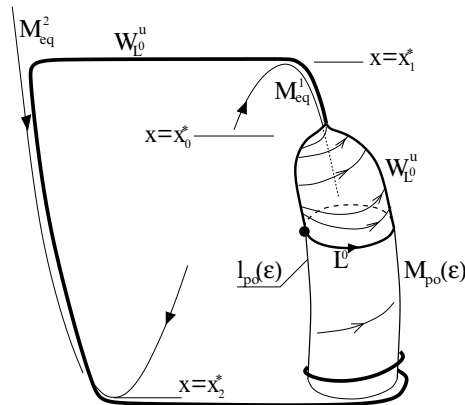


FIGURE 7. The surface M_{po} shrinks into M_{eq}^1 through the supercritical Andronov–Hopf bifurcation in the fast subsystem at $x = x_0^*$.

The third situation (see Fig. 8) corresponds to the case where the stable periodic orbit of the fast system becomes a homoclinic loop of a saddle equilibrium with one-dimensional unstable manifold. Thus, at this value of x , the stable branch of M_{po} terminates by touching a saddle branch of M_{eq} .

At $\varepsilon = 0$, this branch of M_{eq} comprises saddle equilibria of the fast system. The union (over an interval of values of x) of their one-dimensional unstable manifolds

gives a two-dimensional invariant manifold $W^u(M_{\text{eq}})$, and the union of their stable manifolds forms an n -dimensional invariant manifold $W^s(M_{\text{eq}})$. The manifold $W^u(M_{\text{eq}})$ is exponentially attracting, and the manifold $W^s(M_{\text{eq}})$ is exponentially repelling. Both are normally-hyperbolic invariant manifolds and, hence, persist for all sufficiently small ε [3]. The saddle branch $M_{\text{eq}}(\varepsilon)$ is the intersection of $W^u(M_{\text{eq}})$ and $W^s(M_{\text{eq}})$. The manifold $W^u(M_{\text{eq}})$ attracts orbits, so for every initial point close to M_{eq} , the orbit (may be after some drift along M_{eq}) leaves a small neighborhood of M_{eq} close to $W^u(M_{\text{eq}})$, i. e., it leaves M_{eq} at some x and follows one of the separatrices of the corresponding saddle of the fast subsystem.

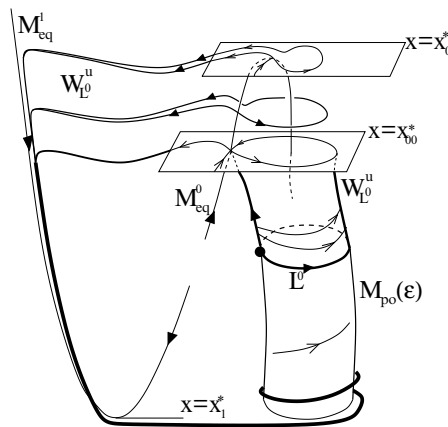


FIGURE 8. The surface M_{po} ends at $x = x_{00}^*$, which corresponds to a homoclinic loop in the fast subsystem. The saddle branch M_{eq}^0 terminates at the fold at $x = x_0^*$. All the orbits starting near M_{eq}^0 arrive eventually to the next stable branch M_{eq}^1 .

3. BLUE-SKY CATASTROPHE

Now, let us suppose that there exists numbers x_0^*, \dots, x_k^* such that the following holds. Our singularly perturbed system has branches $M_{\text{eq}}^1, \dots, M_{\text{eq}}^k$ composed of exponentially stable equilibria of the fast system at $\varepsilon = 0$. Each branch M_{eq}^j is given by the equation $y = y_{\text{eq}}^j(x)$ at $\varepsilon = 0$, where the function $y_{\text{eq}}^j(x)$ is defined on a certain interval of values of x , including the interval between x_{j-1}^* and x_j^* . The drift along the M_{eq}^j is directed from x_{j-1}^* towards x_j^* , i. e.,

$$g(x, y_{\text{eq}}^j(x), 0) \neq 0 \quad \text{and} \quad \text{sign } g(x, y_{\text{eq}}^j(x), 0) = \text{sign}(x_j^* - x_{j-1}^*)$$

for all $x \in [x_{j-1}^*, x_j^*]$ (see (4)). At $x = x_j^*$, the branch M_{eq}^j ends up (namely, it collides with a saddle one); so the fast system has a saddle-node equilibrium at $x = x_j^*$. The unstable manifold of this saddle-node tends to the exponentially stable equilibrium of the fast system on the branch M_{eq}^{j+1} at $j < k$. When $j = k$, the unstable manifold of the saddle-node tends to an exponentially stable periodic

orbit of the fast system. The corresponding stable branch M_{po} extends in x until one of the three following events occurs.

(I) At $x = x_0^*$, the stable branch M_{po} meets that of saddle periodic orbits, i. e., the fast system has a saddle-node periodic orbit. The unstable manifold of this orbit in the fast system tends, as a whole, to the exponentially stable equilibrium on the branch M_{eq}^1 (Fig. 6).

(II) At $x = x_0^*$, the stable periodic orbit of the fast system shrinks to the equilibrium state lying in the branch M_{eq}^1 (Fig. 7).

(III) At some $x = x_{00}^*$ between x_k^* and x_0^* , the stable periodic orbit of the fast system adheres to a homoclinic loop of the saddle equilibrium of the fast system. The corresponding saddle branch M_{eq}^0 extends in x until $x = x_0^*$, where it terminates at the fold representing a saddle-node equilibrium in the fast system; the direction of the shift in x on M_{eq}^0 is from x_{00}^* towards x_0^* . For every x between x_{00}^* and x_0^* , both the one-dimensional separatrices of the saddle of the fast system tend to the stable equilibrium on the branch M_{eq}^1 (at $x = x_{00}^*$, when one of the separatrices forms a homoclinic loop, the other tends to the equilibrium on M_{eq}^1). At $x = x_0^*$, the whole unstable set of the saddle-node of the fast system tends to the exponentially stable equilibrium on M_{eq}^1 (Fig. 8).

In the last case, we need one more assumption. Let $\lambda^j(x)$ stand for maximum of the real part of the characteristic exponents (i. e., for the largest Lyapunov exponent) of the equilibrium state of the fast system for the fixed value of x on the branch M_{eq}^j at $\varepsilon = 0$. By construction, all $\lambda^1(x), \dots, \lambda^k(x)$ are negative (because the equilibria on the branches $M_{eq}^1, \dots, M_{eq}^k$ are exponentially stable). Since the single branch M_{eq}^0 corresponds to a saddle equilibrium, it follows that $\lambda^0(x) > 0$. We assume that

$$\sum_{j=2}^k \int_{x_{j-1}^*}^{x_j^*} \lambda^j(x) \frac{dx}{g(x, y_{eq}^j(x), 0)} + \max_x \left(\int_x^{x_1^*} \lambda^1(x) \frac{dx}{g(x, y_{eq}^1(x), 0)} + \int_{x_{00}^*}^x \lambda^0(x) \frac{dx}{g(x, y_{eq}^0(x), 0)} \right) < 0, \quad (7)$$

where the maximum is taken over all $x \in [x_{00}^*, x_0^*]$.

About the motion near the manifold M_{po} , in all the three cases, we assume also that the function $\phi(x)$ that defines, to the first order, the direction of the drift along M_{po} (see (6)) has constant sign (the same as the sign of $x_0^* - x_k^*$) everywhere except at one point $x = x^{**}$, where ϕ vanishes. So, $\phi(x^{**}) = 0$, $\phi'(x^{**}) = 0$, and we may assume that $\phi''(x^{**}) \neq 0$ (the functions g and h in (1) are required to be at least C^2 -smooth). Let us include our slow-fast system in a one-parameter family of systems (i. e., assume that the functions g and h depend on some parameter μ varying near $\mu = 0$) such that $\phi(x^{**}) = 0$ at $\mu = 0$ and $\frac{\partial \phi}{\partial \mu}(x^{**}) > 0$.

It follows that there exists a smooth curve $\mu = \mu^*(\varepsilon)$, $\mu^*(0) = 0$, such that the function ψ from (6) has exactly two zeros at $\mu < \mu^*(\varepsilon)$, which collide at $\mu = \mu^*(\varepsilon)$, and is non-zero for all x between x_k^* and x_0^* (between x_k^* and x_{00}^* in case III) at $\mu > \mu^*(\varepsilon)$. The zeros of ψ are the fixed points of the Poincaré map on the attracting

invariant manifold $M_{\text{po}}(\varepsilon)$. Thus, if $\mu < \mu^*(\varepsilon)$, then system (2) (or (1)) has two periodic orbits on $M_{\text{po}}(\varepsilon)$, a stable orbit L^+ and a saddle orbit L^- (see Fig. 9).

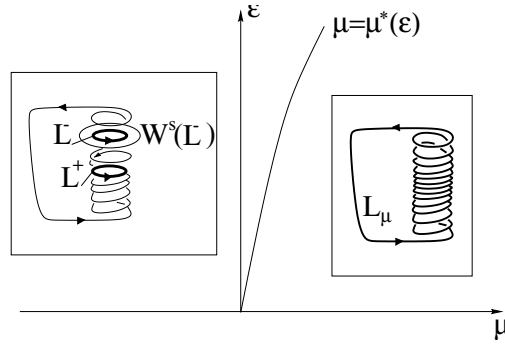


FIGURE 9. At $\mu < \mu^*(\varepsilon)$, the system has two periodic orbits: a stable orbit L^+ and a saddle orbit L^- . The orbits which do not lie in the stable manifold of L^- tend to L^+ as time increases. At $\mu > \mu^*(\varepsilon)$ the system has a single and attracting limit cycle L_μ , whose length tends to infinity as $\mu \rightarrow \mu^*(\varepsilon) + 0$.

Let U be a small fixed neighborhood enveloping the branches M_{po} and M_{eq}^j , as well as the orbits of the fast system which connect them. By construction, every orbit (except those in the stable manifold of L^-) within U tends to L^+ as time increases. Indeed, any orbit which begins near M_{po} and reaches the threshold $x = x_0^*$ or $x = x_{00}^*$, will eventually jump to the next branch M_{eq}^1 ; then, it will drift along it before making the next leap to the similar branch M_{eq}^2 , and so forth, until it will come finally back to the initial branch M_{po} , landing in the attraction basin of the periodic orbit L^+ .

At $\mu = \mu^*(\varepsilon)$, the orbits L^+ and L^- unite into a saddle-node periodic orbit L^0 . The manifold $M_{\text{po}}(\varepsilon)$ is a center manifold for this orbit; the part of $M_{\text{po}}(\varepsilon)$ where the orbits run away from L^0 with increasing time is the unstable manifold of L^0 . After approaching the critical value of x , where the stable branch M_{po} ends, all the orbits on the unstable manifold land closely next to the branch M_{eq}^1 , so that the manifold W_L^u concentrates in a very narrow tube following around and bouncing amongst the slow motion branches M_{eq}^j , prior its final return to L^0 twirling around M_{po} . This gives exactly the configuration of the unstable manifold which was projected in Fig. 2. Therefore, we should anticipate the blue-sky catastrophe here; it occurs indeed according to the following theorem.

Theorem. *In any of cases I, II, and III, for all sufficiently small $\varepsilon > 0$ and $\mu > \mu^*(\varepsilon)$, in the neighborhood U , there exists a unique stable periodic orbit L_μ which attracts all orbits from U . Both the period and the length of L_μ tend to infinity as $\mu \rightarrow \mu^*(\varepsilon) + 0$.*

Proof. By assumption, at $\varepsilon = 0$ and $\mu = 0$, the fast system has a periodic orbit L^0 at $x = x^{**}$. Since L^0 is an exponentially stable periodic orbit of the fast subsystem,

the absolute value of each of its multipliers is less than 1. In the augmented slow-fast system (2), this orbit has an additional multiplier equal to +1 and corresponding to the x variable. Formally, L^0 is a non-hyperbolic periodic orbit of (2) with center variable x . It is well known that such an orbit has an invariant center manifold and an invariant strong-stable foliation which is transverse to the center manifold. Moreover, both persist for all close values of parameters. The center manifold coincides with the surface M_{po} ; so it can be parameterized by the x variable and by the angular variable $\varphi \in \mathbb{S}^1$ (which is indeed the phase on the periodic orbit in the fast system). The flow is uniformly exponentially contracting in the directions transverse to M_{po} . Let us denote the coordinates in these contracting dimensions by $z \in \mathbb{R}^{n-1}$; we can always introduce the z coordinates in such a way that the center manifold becomes locally straightened, i. e., near L_0 , M_{po} has the equation $z = 0$ for all small ε and μ .

The existence of the strong-stable invariant foliation implies that the variables (x, φ, z) in a small neighborhood of L^0 can be introduced in such a way that the evolution of the (x, φ) variables will become independent of the z variable for all small ε and μ (see [10] for details and proofs). Thus, the Poincaré map of an appropriate cross-section, say, $\varphi = 0$, is written near L^0 as

$$\bar{x} = x + \varepsilon\psi(x, \varepsilon, \mu), \quad \bar{z} = A(x, z, \varepsilon, \mu)z, \tag{8}$$

where ψ is the function from (6) and A is an $(n - 1) \times (n - 1)$ matrix such that $\|A\| < 1$.

By assumption, when $\mu > \mu^*(\varepsilon)$, the function ψ vanishes nowhere; for definiteness, we may assume that $\psi > 0$ (in other words, $x_0^* > x_k^*$). Hence, for fixed $x^+ > x^{**}$, any trajectory beginning in a small neighborhood of $x = x^{**}$ will eventually hit the cross-section at a point (x, z) within the strip Σ^+ defined by $x^+ \leq x < x^+ + \varepsilon\psi(x^+, \varepsilon, \mu)$. As time increases, the orbit moves in the direction of increasing x , then it leaps onto a branch M_{eq} , etc.; finally, as explained above, it returns into a small neighborhood of $x = x^{**}$ on M_{po} from the side of $x < x^{**}$. Hence, for any fixed $x^- < x^{**}$ near x^{**} , the orbit will pierce the strip $\Sigma^-: x^- \leq x < x^- + \varepsilon\psi(x^-, \varepsilon, \mu)$ on the cross-section at some uniquely determined point. Thus, the flow outside a small neighborhood of L^0 determines a map $\Sigma^+ \rightarrow \Sigma^-$, which we denote by T_1 .

Similarly, the flow near M_{po} in the region $x^- \leq x < x^+ + \varepsilon\psi(x^+, \varepsilon, \mu)$ defines a map $T_0: \Sigma^- \rightarrow \Sigma^+$ for $\mu > \mu^*(\varepsilon)$. The composition $T_1 \circ T_0$ is a Poincaré map of Σ^- . We will show below that this map is a contraction and hence has a single and stable fixed point attracting all other orbits. This fixed point corresponds to the sought periodic orbit L_μ of the slow-fast system. The number of iterations of the map (8) required to take an orbit from Σ^- to Σ^+ tends to infinity as $\mu \rightarrow \mu^*(\varepsilon) + 0$; each iterate of the map corresponds to one complete revolution of the trajectory of the flow around M_{po} , i. e., to a non-zero length interval on L_μ . Consequently, the total length of L_μ increases without bound as $\mu \rightarrow \mu^*(\varepsilon) + 0$. Thus, to prove the theorem, it is sufficient to evince the contraction of the map $T_1 \circ T_0$.

First, let us show that the first derivative of the map T_0 is uniformly bounded from above. As mentioned, the map is contracting in z , so we have only to check the boundedness of the derivative of the map in the x -variable (which is independent

of z). Take any $x_0 \in [x^-, x^- + \varepsilon\psi(x^-, \varepsilon, \mu)]$ and let $\{x_1, \dots, x_m\}$ be its orbit, i. e., $x_{j+1} = x_j + \varepsilon + \psi(x_j, \varepsilon, \mu)$, and $x_m \in [x^+, x^+ + \varepsilon\psi(x^-, \varepsilon, \mu)]$. We need to prove the uniform boundedness of $\frac{dx_m}{dx_0}$ for arbitrarily large m .

Note that $\frac{dx_{j+1}}{dx_0} = (1 + \varepsilon\psi'(x_j))\frac{dx_j}{dx_0}$ (we do not indicate the dependence of ψ on ε and μ). Following [12], we introduce $\xi_j = \ln \frac{1}{\psi(x_j)} \frac{dx_j}{dx_0}$. It is easy to see that

$$\xi_{j+1} = \xi_j + \ln \frac{(1 + \varepsilon\psi'(x_j))\psi(x_j)}{\psi(x_j + \varepsilon\psi(x_j))} \leq \xi_j + \ln \frac{1 + \varepsilon\psi'(x_j)}{1 + \varepsilon \min_{x \in [x_j, x_{j+1}]} \psi'(x)}.$$

It follows that

$$\xi_{j+1} - \xi_j \leq K\varepsilon(x_{j+1} - x_j),$$

where K is some constant. Hence

$$\xi_m - \xi_0 \leq K\varepsilon(x_m - x_0) \sim K\varepsilon(x^+ - x^-).$$

Thus, $\xi_m - \xi_0$ is uniformly bounded, which means that $\frac{\psi(x_0)}{\psi(x_m)} \frac{dx_m}{dx_0}$ is uniformly bounded too. Since x_0 is bounded away from x^{**} , the value of $\psi(x_0)$ is also bounded away from zero, which implies the required uniform boundedness of $\frac{dx_m}{dx_0}$.

Next, we shall prove that the map T_1 is contracting with contraction factor tending to zero as $\varepsilon \rightarrow +0$ for all μ . Choose a point $M \in \Sigma^+$ and put $\bar{M} = T_1 M \in \Sigma^-$. The phase velocity vectors (\dot{x}, \dot{y}) at both endpoints M and \bar{M} are bounded away from zero and the angle between these vectors and the cross-section is bounded away from zero as well for all small ε ; therefore, to prove the strong contraction property for the map T_1 , it is sufficient to show that the flow from M to \bar{M} contracts strongly two-dimensional areas for any initial point $M \in \Sigma^+$. To do this, we split the flight from Σ^+ to Σ^- into a few stages, namely, a slow drift along M_{po} , jumps towards and between the branches M_{eq} , slow passages along these branches, and the final leap back to M_{po} together with the drift along it until reaching Σ^- . Let us pick a sufficiently small $\delta > 0$. The interval of time (τ) needed for a trajectory of system (2) to fly from the δ -neighborhood of one branch to the δ -neighborhood of the other branch is finite. Therefore, every such jump brings only a finite contribution into the contraction or expansion of areas. The number of such interbranch leaps is finite too, so altogether the jumps can contribute only a finite factor to the overall expansion/contraction of areas.

The first two Lyapunov exponents of the trajectory of the unperturbed system (2) at a point x on M_{eq}^j are 0 and $\lambda^j(x)$ when $\varepsilon = 0$ (the zero exponent corresponds to the x variable, whereas λ^j is determined by the fast system). Therefore, when ε is nonzero and small, the time- $\Delta\tau$ shift ($\Delta\tau$ is small enough) set by the flow in the δ -neighborhood of the point x multiplies the areas by a factor bounded above by $e^{(\lambda^j(x) + O(\delta) + O(\varepsilon))\Delta\tau}$. It follows that the total coefficient of expansion or contraction of areas gained during the transport in the δ -neighborhood of the branch M_{eq}^j from

a point x_1 to a point x_2 is bounded above by

$$C_1 \exp\left(\frac{1}{\varepsilon} \int_{x_1}^{x_2} (\lambda^j(x) + C_2\delta) \frac{dx}{g(x, y_{\text{eq}}^j(x), 0)}\right),$$

where $C_{1,2}$ are some constants independent of x , δ , and ε . Recall that $\lambda^j < 0$ for $j = 1, \dots, k$. Thus, if $\delta > 0$ is sufficiently small, in any of cases I, II, and III (in case III, inequality (7) is crucial), during the phase of motion between Σ^+ and Σ^- which corresponds to the drift in the δ -neighborhood of the branches M_{eq}^j and the interbranch jumps, the flow contracts areas with a factor at least $e^{-\alpha/\varepsilon}$, where $\alpha > 0$ is a constant independent of δ and ε .

Now, note that the flow in the δ -neighborhood of M_{po} but outside a small neighborhood of $x = x^{**}$ and the δ -neighborhood of the branches M_{eq} cannot produce a strong expansion of areas. Indeed, the first two Lyapunov exponents for system (2) at $\varepsilon = 0$ are both zero on M_{po} (as above, the first one corresponds to the x variable and the other to the circular motion on the stable periodic orbit of the fast system). In fact, every complete revolution in the δ -neighborhood of M_{po} but outside the δ -neighborhood of the branches M_{eq} results in an area expansion at rate estimated as $e^{O(\delta)}$. When $\varepsilon \neq 0$ is sufficiently small, this estimate becomes only slightly worse, namely, the factor becomes $e^{O(\delta)+O(\varepsilon)}$. The number of the turns that the orbit makes around M_{po} while travelling along the path from Σ^- towards Σ^+ (i. e., outside a small neighborhood of x^{**}) is evaluated as $O(\varepsilon^{-1})$ (because the function ψ is bounded away from zero in this region; see (6)). Hence the factor of possible expansion of areas accumulating during the phase of transport from Σ^+ to Σ^- which corresponds to the drift near M_{po} does not exceed some $e^{C(1+\frac{\delta}{\varepsilon})}$.

Thus, when ε is small enough, the areas are indeed strongly contracted during the flight from Σ^+ to Σ^- . Hence, the map T_1 is a strong contraction, and so is the map $T_1 \circ T_0: \Sigma^- \rightarrow \Sigma^-$. This completes the proof of the theorem. \square

4. SUMMARY

To conclude, we emphasize that the suggested mechanisms of the blue-sky catastrophe in slow-fast systems have indeed been observed in models of neuronal activity, describing the dynamics of the leech heart neurons; see [7]. In both cases, the smooth transition (illustrated in Fig. 9) from one type of self-sustained oscillations (the round stable periodic orbit L^+) to the regime where the attractor is the “long” stable orbit L_μ can be interpreted as a transition from periodic tonic-spikes to periodic bursting oscillations. Here, each burst is constituted by the slow helix-like motion along M_{po} generating a large number of spikes followed by the inter-burst “calm” phase due to the sluggish drive along M_{eq} .

Note also that, even before the transition to the bursting oscillations, the spiking mode is in excitable state: a perturbation which drives the initial point outside the saddle limit cycle L^- results in a long calm phase before the sustained spiking restores.

REFERENCES

- [1] A. A. Andronov and E. A. Leontovich, *Some cases of dependence of limit cycles on a parameter*, Uchenye zapiski Gorkovskogo Universiteta **6** (1937), 3–24.
- [2] A. A. Andronov, E. A. Leontovich, I. I. Gordon, and A. G. Maier, *Theory of bifurcations of dynamic systems on a plane*, Halsted Press [A division of John Wiley & Sons], New York-Toronto, Ont., 1973. MR [0344606](#).
- [3] N. Fenichel, *Persistence and smoothness of invariant manifolds for flows*, Indiana Univ. Math. J. **21** (1971/1972), 193–226. MR [0287106](#)
- [4] N. Fenichel, *Geometric singular perturbation theory for ordinary differential equations*, J. Differential Equations **31** (1979), no. 1, 53–98. MR [80m:58032](#)
- [5] N. Gavrilov and A. Shilnikov, *Example of a blue sky catastrophe*, Methods of qualitative theory of differential equations and related topics, Amer. Math. Soc. Transl. Ser. 2, vol. 200, Amer. Math. Soc., Providence, RI, 2000, pp. 99–105. MR [2001g:37076](#)
- [6] L. S. Pontryagin and L. V. Rodygin, *Periodic solution of a system of ordinary differential equations with a small parameter in the terms containing derivatives*, Dokl. Akad. Nauk SSSR **132** (1960), 537–540 (Russian). MR [0120426](#). English translation: Soviet Math. Dokl. **1** (1960), 611–614.
- [7] A. L. Shilnikov and G. Cymbalyuk, *Transition between tonic-spiking and bursting in a neuron model via the blue-sky catastrophe*, Phys. Review Letters, **94** (2005), 048101; A. L. Shilnikov and G. Cymbalyuk, *Homoclinic saddle-node orbit bifurcations en a route between tonic spiking and bursting in neuron models*, Regul. Dynamics **9** (2004), no. 3, 281–297. MR [2104173](#)
- [8] L. P. Shilnikov, *Some cases of generation of period motions from singular trajectories*, Mat. Sb. (N.S.) **61(103)** (1963), 443–466 (Russian). MR [0153916](#)
- [9] L. P. Shilnikov, A. L. Shilnikov, D. Turaev, and L. O. Chua, *Methods of qualitative theory in nonlinear dynamics. Part II*, World Scientific Series on Nonlinear Science. Series A: Monographs and Treatises, vol. 5, World Scientific Publishing Co. Inc., River Edge, NJ, 2001. MR [2003d:37002](#)
- [10] L. P. Shilnikov, A. L. Shilnikov, D. V. Turaev, and L. O. Chua, *Methods of qualitative theory in nonlinear dynamics. Part I*, World Scientific Series on Nonlinear Science. Series A: Monographs and Treatises, vol. 4, World Scientific Publishing Co. Inc., River Edge, NJ, 1998. MR [2000h:37001](#)
- [11] L. P. Shilnikov and D. V. Turaev, *Simple bifurcations leading to hyperbolic attractors*, Comput. Math. Appl. **34** (1997), no. 2-4, 173–193. MR [98i:58179](#)
- [12] L. P. Shilnikov and D. V. Turaev, *A new simple bifurcation of a periodic orbit of “blue sky catastrophe” type*, Methods of qualitative theory of differential equations and related topics, Amer. Math. Soc. Transl. Ser. 2, vol. 200, Amer. Math. Soc., Providence, RI, 2000, pp. 165–188. MR [2001i:37078](#)
- [13] D. V. Turaev and L. P. Shilnikov, *Blue sky catastrophes*, Dokl. Akad. Nauk **342** (1995), no. 5, 596–599 (Russian). MR [96g:58139](#)

DEPARTMENT OF MATHEMATICS AND STATISTICS, GEORGIA STATE UNIVERSITY, 30 PRYOR STREET, ATLANTA 30303, USA

E-mail address: ashilnikov@mathstat.gsu.edu

INSTITUTE FOR APPLIED MATHEMATICS AND CYBERNETICS, 10 ULYANOV STREET, NIZHNY NOVGOROD, 603005 RUSSIA

E-mail address: diffequ@unn.ac.ru

DEPARTMENT OF MATHEMATICS, BEN GURION UNIVERSITY OF THE NEGEV, P.O.B. 653, BE’ER SHEVA 84105, ISRAEL

E-mail address: turaev@math.bgu.ac.il